animals

MDPI

Article

Dietary 5-Aminolevulinic Acid Improves Hepatic Lipid–Redox Homeostasis in Laying Hens by Engaging HO-1

Xuanfu Wu, Haozhou Luo, Lin Peng, Dongxu Zhang and Wenqiang Ma *

Key Laboratory of Animal Physiology and Biochemistry, Ministry of Agriculture and Rural Affairs, College of Veterinary Medicine, Nanjing Agricultural University, Nanjing 210095, China; 2021807150@stu.njau.edu.cn (X.W.); 2024807186@stu.njau.edu.cn (H.L.); 2023007053@stu.njau.edu.cn (L.P.); 2025207008@stu.njau.edu.cn (D.Z.)

* Correspondence: wq8110@njau.edu.cn; Tel.: +86-025-84396413

Simple Summary

Laying hens produce large amounts of fat in the liver to support egg formation, making liver health important for poultry production. Excess fat accumulation and oxidative damage can impair liver function. This study investigated whether adding 5-aminolevulinic acid to the diet could improve the liver fat balance and antioxidant protection. After eight weeks on a standard basal diet, supplemented hens had less liver fat, an improved liver tissue appearance, and stronger antioxidant defenses. In cultured chicken liver cells exposed to fatty acids, the compound also reduced fat accumulation and oxidative damage and improved the cellular energy status. Reducing the expression of heme oxygenase 1 weakened these protective effects. These findings identify 5-aminolevulinic acid as a potential nutritional approach for supporting liver health in laying hens and provide a basis for further studies under different feeding and production conditions.

Abstract

This study first evaluated the effects of dietary 5-aminolevulinic acid (5-ALA) on hepatic lipid metabolism and the antioxidant status in an eight-week feeding trial in Hy-Line Brown laying hens receiving a standard basal diet. Subsequent experiments in palmitic/oleic acid (PA/OA)-challenged leghorn male hepatoma (LMH) cells examined the hepatocellular response and the contribution of heme oxygenase 1 (HO-1). Hens receiving 20 mg/kg 5-ALA showed lower hepatic triglyceride and cholesterol concentrations, reduced steatosis and lobular inflammation, higher superoxide dismutase activity, and a lower malondialdehyde content. Transcriptomic analysis identified 301 differentially expressed genes, and gene set enrichment analysis showed the positive enrichment of fatty acid degradation, peroxisome, and peroxisome proliferator-activated receptor signaling pathways. Reverse transcription quantitative polymerase chain reaction and Western blotting showed increased HMOX1/HO-1 expression and markers of fatty acid metabolism and mitochondrial function. In PA/OA-challenged LMH cells, 500 μmol/L 5-ALA reduced triglyceride accumulation, lipid droplets, reactive oxygen species, and malondialdehyde, while improving superoxide dismutase activity, adenosine triphosphate levels, and mitochondrial membrane potential. HMOX1 silencing attenuated selected protective responses. Dietary 5-ALA improves hepatic lipid–redox homeostasis under standard feeding conditions, with the subsequent cell experiments supporting a contribution of HO-1 to cytoprotection.

Academic Editor: Chunqi Gao

Received: 25 October 2026
Revised: 13 November 2026
Accepted: 24 November 2026
Published: 26 November 2026

Copyright: © 2026 by the authors. Licensee MDPI, Basel, Switzerland. This article is an open access article distributed under the terms and conditions of the Creative Commons Attribution (CC BY) license.

Keywords: 5-aminolevulinic acid; laying hen; hepatic lipid homeostasis; heme oxygenase 1; fatty acid oxidation; mitochondrial function

1. Introduction

Egg production places sustained and distinctive metabolic demands on the liver of laying hens. Under estrogen stimulation, the liver synthesizes lipids and produces yolk-targeted very-low-density lipoprotein (VLDLy) and vitellogenin (VTG) for delivery to the ovary [1]. The liver must therefore balance lipid synthesis and assembly with oxidation and export while operating under a high lipogenic load. If this balance remains disrupted, lipids accumulate in hepatocytes and fatty liver hemorrhagic syndrome (FLHS) may develop, compromising hen health, productive performance, and welfare [2].

The ability of the liver to accommodate this lipid load depends on coordinated fatty acid catabolism, organelle homeostasis, and redox control. Mitochondria and peroxisomes contribute to fatty acid β-oxidation and related metabolic processes, and their functional adaptation can influence whether lipids are used or retained in the liver [3]. Previous studies in laying hens have linked reduced lipogenesis, increased fatty acid oxidation, or improved mitophagy to lower hepatic lipid deposition and oxidative injury [4–6]. In a high-energy, low-protein diet model of FLHS, dietary coated sodium butyrate reduced hepatic lipid deposition and oxidative stress while attenuating mitochondrial damage and restoring autophagy-related indices in laying hens [7]. These findings support the further evaluation of nutritional interventions that influence lipid utilization, organelle homeostasis, and redox balance in laying hens.

5-Aminolevulinic acid (5-ALA) is generated in the first and generally rate-limiting step of heme biosynthesis, which is catalyzed by 5-aminolevulinate synthase (ALAS) [8]. Heme is an essential prosthetic group in hemoglobin, cytochromes, peroxidases, and other proteins involved in oxygen transport, redox reactions, and mitochondrial electron transfer. This biochemical role has prompted interest in 5-ALA as an animal feed additive. Studies in livestock and poultry have focused largely on iron utilization, hematological traits, immune responses, productive performance, and the quality of animal products [9]. In high-fat diet-fed mice, 5-ALA reduced the hepatic lipid content and increased AMPK phosphorylation, while complementary experiments in HepG2 cells showed higher PGC-1α and CPT1A expression [10]. In palmitate-treated Huh7 hepatocytes, 5-ALA induced heme oxygenase 1 (encoded by *HMOX1*) and attenuated endoplasmic reticulum stress and lipotoxic apoptosis [11]. Poultry studies have also reported increased hepatic HO-1 expression in lipopolysaccharide-challenged broilers and increased renal HO-1 expression in heat-stressed laying hens [12,13].

Although 5-ALA has been reported to attenuate hepatic steatosis in high-fat-diet-fed mice [10], reduce endoplasmic reticulum stress and lipotoxic apoptosis in palmitate-treated Huh-7 cells [11], and induce HO-1 in renal tubular cells [14] and broiler tissues [12], the laying-hen liver represents a fundamentally distinct metabolic context. The laying-hen liver sustains a high lipogenic and oxidative load during egg production [1]. Whether 5-ALA remains effective under this physiological lipid load, whether it engages a coordinated transcriptional program encompassing fatty acid β-oxidation, peroxisomal function, and mitochondrial activity, and whether HO-1 contributes to the hepatocellular response in avian cells remain unresolved. The present study addresses these three gaps by integrating network pharmacology, hepatic RNA-seq, targeted mRNA and protein validation, and HMOX1 siRNA intervention in chicken LMH hepatocytes.

2. Materials and Methods

The study began with a laying hen feeding trial to evaluate hepatic responses to dietary 5-ALA. Liver transcriptomics and targeted biochemical and molecular measurements were used to characterize the in vivo response. Subsequent PA/OA-challenged LMH-cell experiments provided a controlled setting to examine the hepatocellular effects of 5-ALA and the contribution of HO-1 through HMOX1 silencing. The pilot experiment used to select the dietary dose was a separate, preceding feeding trial in laying hens.

2.1. Animal Ethics Statement

The Animal Ethics Committee of Nanjing Agricultural University approved all animal procedures (NJAULLSC2024064), which were conducted in accordance with the applicable Chinese laboratory-animal guidelines.

2.2. Network Pharmacology Analysis

Candidate genes associated with 5-ALA were compiled across species from curated chemical–gene associations in the Comparative Toxicogenomics Database (CTD) and predictions from SwissTargetPrediction, TargetNet, and the Similarity Ensemble Approach (SEA). The original SwissTargetPrediction analysis used Rattus norvegicus [15]. Fatty-liver-associated genes were obtained from CTD (Fatty Liver; MeSH D005234). Records were aggregated by gene symbol, retaining genes with a maximum inference score ≥106.53 and a maximum reference count ≥217, yielding 4045 disease-associated symbols. Intersection with the 279 5-ALA-associated source symbols yielded 155 candidates. Table S4 lists the standardized identifiers and chicken orthologs. Table S5 lists the database sources for each candidate, Table S6 identifies the species represented in the SwissTargetPrediction export, and Table S7 lists the archived SEA predictions.

For the revised reference-network analysis, the 155 source symbols were standardized to 157 human reference genes using official symbols, aliases, and recorded orthology relationships. SCD1 was resolved to SCD, RAC1 was assigned its canonical human Ensembl identifier, and all three returned human orthologs of mouse Cyp2a5 (CYP2A6, CYP2A7, and CYP2A13) were retained. The reference network was recalculated in STRING 12.0 (Homo sapiens; taxonomy ID 9606), using functional associations with a combined score ≥0.700 and no additional interactors. Only nodes with at least one qualifying association were displayed. Selected genes were visually highlighted for their relevance to lipid metabolism and redox regulation.

GO and KEGG enrichment analyses were performed in g:Profiler (g:GOSt, version e114_eg62_p19_9dc92ac8) [16] using unordered queries, species-specific annotated-gene backgrounds, electronic annotations, and g:SCS correction, with adjusted $p < 0.05$ as the significance threshold. For a comparison with the original figure, previously displayed terms were retained when they remained significant. Human reference genes were mapped to Gallus gallus using g:Orth (g:Profiler version e114_eg62_p19_9dc92ac8), retaining returned one-to-many relationships: 131 human genes mapped to 139 unique chicken orthologs, while 26 human genes had no returned chicken mapping. The chicken orthologs were analyzed against the chicken annotated-gene background (ggallus). Table S8 lists the significant enrichment results for chicken orthologs. Table S9 compares enrichment results with and without the seven candidates identified only by SEA.

Chicken Entrez identifiers were used to link ortholog candidates to the liver RNA-seq annotation. The linked candidates were intersected with the 301 differentially expressed genes selected using $p < 0.05$ and $|\log_2 \text{fold change}| \geq 1$. The overlap and the RNA-seq results for HMOX1 and CPT1A are provided in Tables S2 and S3.

2.3. Birds, Diets, and Experimental Design

Two hundred and fifty-two Hy-Line Brown laying hens aged 300 d were used in a single-factor experiment. Based on the pre-trial laying rate, birds were allocated at random to one of two dietary treatments: a basal diet, or the basal diet supplemented with 20 mg/kg 5-ALA. Each treatment comprised six replicate cages of 21 hens. 5-ALA (99% purity) was supplied by Xi'an Tianhe Pharmaceutical Co., Ltd. (Xi'an, Shaanxi, China). Prior to incorporation into the basal diet, 5-ALA was pre-blended thoroughly with the vitamin–mineral premix and then mixed stepwise with the remaining ingredients to ensure a homogeneous distribution.

The dietary inclusion level was selected using a preceding eight-week dose-comparison feeding trial in Hy-Line Brown laying hens. This trial compared 0, 20, 40, and 60 mg/kg dietary 5-ALA, with 126 hens per treatment arranged in six replicates of 21 hens. Dose selection considered the laying rate and feed conversion ratio. The 20 mg/kg group had a higher mean laying rate and a lower feed conversion ratio over the full trial, while increasing the dose to 40 or 60 mg/kg produced no further increase in the laying rate. The lowest tested supplemental level, 20 mg/kg, was therefore selected for the present study.

Following a 7 d adaptation period, the feeding trial was conducted for 8 wk. Birds were housed in stacked cages and fed twice daily (09:00 and 17:00) at 130 g/hen/day, with water available ad libitum; no conspicuous feed refusals were noted. The lighting program provided 16 h of light and 8 h of dark. The corn–soybean meal mash diet was formulated with reference to the NRC (1994) [17] and the Chinese Feeding Standard of Chicken (NY/T 33-2004), as in the study by Chang et al. [18]. The ingredient composition and calculated nutrient levels are shown in Table 1.

Table 1. Composition and nutrient levels of the basal diet for Hy-Line Brown laying hens.

Ingredient	Content, %	Nutrient level	Content
Corn	62.50	Apparent metabolizable energy, MJ/kg	10.43
Soybean meal	23.00	Crude protein, %	15.38
Soybean oil	0.50	Methionine, %	0.35
Limestone	9.00	Lysine, %	0.81
Premix	5.00	Calcium, %	3.92
Total	100.00	Available phosphorus, %	0.27

Note: The premix provided the following per kilogram of diet: vitamin A, 7500 IU; vitamin D3, 4500 IU; vitamin E, 37.5 IU; vitamin K3, 3 mg; thiamine, 6.5 mg; riboflavin, 8.75 mg; niacinamide, 40 mg; pantothenic acid, 15 mg; pyridoxine, 4 mg; folic acid, 1.5 mg; biotin, 0.2 mg; cobalamin, 0.02 mg; choline chloride, 400 mg; Zn, 95 mg; Fe, 100 mg; Cu, 8.75 mg; Mn, 105 mg; Se, 0.25 mg; I, 1.2 mg; Ca, 4 g; P, 2 g; methionine, 1 g; and NaCl, 2 g.

2.4. Sample Collection

At the end of the trial, two hens were selected at random from each replicate cage, giving 12 birds per treatment. After body weight had been recorded, fresh whole blood was drawn for hemoglobin determination. Blood destined for serum preparation was collected without an anticoagulant, allowed to clot at room temperature for 4 h, and centrifuged at 3000 rpm for 10 min; serum was stored at −20 °C until analysis.

Birds were then euthanized via cervical dislocation, and the liver was excised. Portions of the liver were fixed in 4% paraformaldehyde for hematoxylin–eosin (H&E) staining, mounted as frozen sections for Oil Red O staining, or snap-frozen in liquid nitrogen and stored at −80 °C for biochemical and molecular analyses. One representative liver sample from each replicate was used for RNA sequencing, RT-qPCR validation, and matched correlation analyses, giving six biological samples per treatment and 12 samples

in total (six CON and six 5-ALA). Transcript abundance, HMOX1 RT-qPCR expression, and phenotypic measurements were matched by the individual bird for correlation analyses.

2.5. Biochemical Measurements in Serum, Whole Blood, and Liver

Serum alanine aminotransferase (ALT) and aspartate aminotransferase (AST) activities were measured using commercial reagents from MedicalSystem Biotechnology Co., Ltd. (Ningbo, Zhejiang, China) on a Hitachi 7020 automated biochemical analyzer (Hitachi High-Technologies Corp., Tokyo, Japan), and the AST/ALT ratio was calculated. Serum triglyceride (TG) and total cholesterol (TC) were determined using commercial kits from Nanjing Jiancheng Bioengineering Institute (Nanjing, Jiangsu, China). Hemoglobin in fresh whole blood was measured using a commercial kit (C021; Nanjing Jiancheng Bioengineering Institute).

Liver tissue was homogenized under chilled conditions, and the supernatant was collected after centrifugation. Hepatic TG was determined with a kit (Nanjing Jiancheng). Hepatic TC and free cholesterol (FC) were measured with kits (Applygen Technologies, Beijing, China), and cholesteryl ester (CE) was calculated as CE = TC − FC. Hepatic SOD activity and MDA content were determined with kits (Nanjing Jiancheng). All assays followed the manufacturers' instructions, and values were normalized as indicated in the corresponding figures.

2.6. Liver Histology and Scoring

Fixed liver tissue was paraffin embedded, sectioned, and stained with H&E. Separate frozen sections were stained with Oil Red O and counterstained with hematoxylin to assess neutral-lipid deposition. Images were acquired using a PANNORAMIC MIDI digital slide scanner (3DHISTECH Kft., Budapest, Hungary).

Histological scoring was performed with the assessors blinded to the treatment groups. Steatosis, lobular inflammation, and hepatocellular ballooning were assessed according to the scoring framework described by Kleiner et al. [19]. Steatosis was scored as 0 (<5%), 1 (5% to 33%), 2 (>33% to 66%), or 3 (>66%); lobular inflammation was scored as 0 (none), 1 (<2 foci per 200× field), 2 (2 to 4 foci per 200× field), or 3 (>4 foci per 200× field); and ballooning was scored as 0 (none), 1 (few ballooned cells), or 2 (many or prominent ballooned cells). No evident hepatocellular ballooning was observed in either treatment; therefore, both groups received a ballooning score of 0, and this component was not plotted separately.

2.7. Liver RNA Sequencing and Bioinformatic Analysis

Twelve liver samples, comprising six per treatment with one sample from each replicate cage, were subjected to transcriptome sequencing by Shanghai Personal Biotechnology Co., Ltd. (Shanghai, China). Total RNA was extracted using TRIzol reagent (Thermo Fisher Scientific, Waltham, MA, USA). The RNA concentration was measured with a NanoDrop ND-1000 spectrophotometer (Thermo Fisher Scientific, Wilmington, DE, USA), and RNA integrity was evaluated with an Agilent 2100 Bioanalyzer (Agilent Technologies, Santa Clara, CA, USA). Samples with an RNA concentration >50 ng/μL, RNA integrity number >7.0, and total RNA yield >1 μg were used for library preparation.

Poly(A)+ mRNA was enriched through 2 rounds of purification with Dynabeads Oligo(dT)25 (Thermo Fisher Scientific). The enriched mRNA was fragmented at 94 °C for 5 to 7 min using the NEBNext Magnesium RNA Fragmentation Module (New England Biolabs, Ipswich, MA, USA). First-strand cDNA was synthesized using SuperScript II reverse transcriptase (Thermo Fisher Scientific), followed by second-strand synthesis with *Escherichia coli* DNA polymerase I (New England Biolabs), RNase H (New England

Biolabs), and dUTP (Thermo Fisher Scientific). After end repair, A-tailing, adapter ligation, and size selection, libraries were treated with uracil-DNA glycosylase (New England Biolabs). PCR amplification was performed at 95 °C for 3 min; 8 cycles of 98 °C for 15 s, 60 °C for 15 s, and 72 °C for 30 s; and 72 °C for 5 min. Libraries with an average insert size of 300 ± 50 bp were sequenced on an Illumina NovaSeq 6000 platform (Illumina, Inc., San Diego, CA, USA) using 150 bp paired-end reads.

Raw reads were filtered with fastp to remove adapters and low-quality reads. Clean reads were aligned to the chicken reference genome using HISAT2, and gene-level counts were generated in Union mode with HTSeq. Gene expression was expressed as fragments per kilobase of transcript per million mapped reads. Sample reproducibility and overall expression patterns were evaluated via Pearson correlation and principal component analysis. Differential expression was analyzed using DESeq2, with $p < 0.05$ and $|\log2 \text{ fold change}| \geq 1$ as the thresholds. GO and KEGG enrichment analyses of differentially expressed genes were performed using one-sided hypergeometric tests in SciPy (version 1.17.1), with $p < 0.05$ as the reporting threshold. Gene set enrichment analysis was conducted using a preranked gene list, with $|\text{normalized enrichment score}| > 1$, $p < 0.05$, and false discovery rate $q < 0.25$ as the prespecified thresholds; the FDR of each displayed gene set was also reported.

2.8. Reverse Transcription Quantitative Polymerase Chain Reaction

Total RNA from liver tissue or LMH cells was extracted using TransZol Up reagent (TransGen Biotech Co., Ltd., Beijing, China). The RNA concentration and purity were determined using a GeneQuant 1300 spectrophotometer (Biochrom Ltd., Cambridge, UK). Equal quantities of RNA were reverse transcribed using TransScript Uni All-in-One First-Strand cDNA Synthesis SuperMix with genomic DNA removal (TransGen Biotech).

Quantitative PCR was performed with ChamQ SYBR qPCR Master Mix (Vazyme Biotech Co., Ltd., Nanjing, Jiangsu, China) on a CFX384 Touch Real-Time PCR Detection System (Bio-Rad Laboratories, Hercules, CA, USA). The program comprised 95 °C for 30 s, followed by 40 cycles of 95 °C for 5 s and 60 °C for 30 s. β-Actin was used as the reference gene, and relative expression was calculated using the $2^{-\Delta\Delta Ct}$ method. The genes examined were *CPT1A*, *HMOX1*, *ACAA1*, *ACSL1*, *PPARGC1A*, *TFAM*, *TOMM20*, and *SDHB*. Primers were synthesized by Tsingke Biotechnology Co., Ltd. (Nanjing, Jiangsu, China), and the sequences are listed in Table 2.

Table 2. Primer sequences used for RT-qPCR.

Gene	Accession number	Forward primer (5′–3′)	Reverse primer (5′–3′)
ACSL1	NM_001012578	ACCGGTCTGTGCGTTGTTG	CGAGCATCCTCTTCACCCTC
CPT1A	NM_001012898	TGAGCACTCTTGGGCAGATG	TCTCCTTTGCAGTGTCCGTC
PPARGC1A	NM_001006457.2	GACATGTGCAACCAGGACTCT	GGTCAAGTTCTGGGAGGTCTG
ACAA1	NM_001197288	AACAGCAAAGCTCGCGATTG	GCTTTGCCAAACCTTCCAGG
HMOX1	NM_205344.2	AGCTTCGCACAAGGAGTGTT	GGAGAGGTGGTCAGCATGTC
TFAM	NM_204100.2	CCAGCAGAACCCAGAACTGAA	CTGTCTTCCTTGCTTCCTCGT
TOMM20	XM_423972.8	AGCCAGAGAATTGTAAGTGCACA	CTGATGCTCATCTTCTGGGGT
SDHB	NM_001080875.3	GTCAGAAACTGGACGGACTCT	CAGGACCCAAGTACTTGTCCC
ACTB	NM_205518	TGCTGTGTTCCCATCTATCG	TTGGTGACAATACCGTGTTCA

Abbreviations: ACSL1, acyl-CoA synthetase long-chain family member 1; CPT1A, carnitine palmitoyltransferase 1A; PPARGC1A, peroxisome proliferator-activated receptor gamma coactivator 1-alpha; ACAA1, acetyl-CoA acyltransferase 1; HMOX1, heme oxygenase 1; TFAM, mitochondrial transcription factor A; TOMM20, translocase of outer mitochondrial membrane 20; SDHB, succinate dehydrogenase complex iron sulfur subunit B; ACTB, actin beta. β-Actin (ACTB) was used as the reference gene for RT-qPCR normalization. F, forward; R, reverse.

2.9. Western Blotting

Approximately 50 mg of liver tissue was homogenized in 500 μL RIPA lysis buffer containing 1% phenylmethylsulfonyl fluoride and lysed on ice for 60 min, with 20 s mixing every 15 min. LMH cells were washed with precooled phosphate-buffered saline and lysed in RIPA buffer. After centrifugation, the supernatant was collected and the protein concentration was determined using a bicinchoninic acid (BCA) assay.

Based on the BCA measurements, approximately 50 μg of total protein per lane was mixed with 5× loading buffer, heated at 100 °C for 10 min, separated via 10% SDS-PAGE, and transferred to nitrocellulose membranes. Membranes were blocked with 5% skim milk, incubated with primary antibodies overnight at 4 °C, washed, and incubated with a horseradish peroxidase-conjugated secondary antibody for 2 h at room temperature. Immunoreactive bands were detected using enhanced chemiluminescence, and densitometry was performed with ImageJ 1.51 (National Institutes of Health, Bethesda, MD, USA).

Liver samples were analyzed for HO-1, CPT1A, ACAA1, ACSL1, PGC-1α, TFAM, TOM20, and SDHB. PA/OA-treated LMH cells were analyzed for HO-1, CPT1A, ACAA1, ACSL1, PGC-1α, TFAM, cytochrome c oxidase subunit IV (COXIV), and mitofusin 2 (MFN2), with α-tubulin as the loading control. The *HMOX1*-silencing experiments included CPT1A, ACAA1, PGC-1α, TFAM, and TOM20. Antibody information is provided in Table 3. The original Western blot images are provided in the Supplementary Materials.

Table 3. Antibodies used for Western blotting.

Target	Supplier	Catalogue no.	Dilution
ACAA1	ABclonal Technology, Wuhan, China	A25034	1:1000
CPT1A	Proteintech Group, Rosemont, IL, USA	15184-1-AP	1:1000
ACSL1	Proteintech Group	13989-1-AP	1:1000
PGC-1α	ABclonal Technology	A20995	1:1000
SDHB	Proteintech Group	10620-1-AP	1:10,000
COXIV	Proteintech Group	11242-1-AP	1:10,000
MFN2	Proteintech Group	12186-1-AP	1:2000
TOM20	Proteintech Group	11802-1-AP	1:5000
HO-1	Proteintech Group	10701-1-AP	1:1000
TFAM	ABclonal Technology	A3173	1:2000
GAPDH	Proteintech Group	10494-1-AP	1:10,000
α-Tubulin	Bioworld Technology, Nanjing, China	BS1699	1:10,000
Rabbit IgG (secondary antibody)	Bioworld Technology	BS13278	1:10,000

Abbreviations: ACAA1, acetyl-CoA acyltransferase 1; CPT1A, carnitine palmitoyltransferase 1A; ACSL1, acyl-CoA synthetase long-chain family member 1; PGC-1α, peroxisome proliferator-activated receptor gamma coactivator 1-alpha; SDHB, succinate dehydrogenase complex iron sulfur subunit B; COXIV, cytochrome c oxidase subunit IV; MFN2, mitofusin 2; TOM20, translocase of outer mitochondrial membrane 20; HO-1, heme oxygenase 1; TFAM, mitochondrial transcription factor A; GAPDH, glyceraldehyde-3-phosphate dehydrogenase; α-tubulin, alpha-tubulin. GAPDH and α-tubulin were used as loading controls, and target-protein signals were normalized to the corresponding loading control. The secondary antibody was HRP-conjugated goat anti-rabbit IgG (H+L). IgG, immunoglobulin G; HRP, horseradish peroxidase; H+L, heavy and light chains.

2.10. Correlation Analysis

Correlation analyses pooled the 12 individual birds represented in the liver transcriptome dataset (six CON and six 5-ALA; one bird per replicate cage). Whole-blood hemoglobin and hepatic TG, MDA, SOD, TC, FC, and CE measurements were matched to the

transcriptomic profile and HMOX1 RT-qPCR expression of the same bird. Each correlation therefore used 12 matched observations.

Spearman rank correlations were used to examine pairwise associations among HMOX1, phenotypic variables, and lipid-metabolism-related differentially expressed genes. Two-sided p values were used. Genes were ranked by the number of associations with $p < 0.05$, then by the minimum p value and maximum absolute correlation, and the first 18 genes were selected for visualization. Edges meeting $p < 0.05$ and $|\varrho| \geq 0.58$ were ranked by ascending p value and descending $|\varrho|$, with up to 46 edges displayed. The $|\varrho|$ threshold and display limits controlled network density. Mantel tests were used to evaluate associations of HMOX1 expression or the combined expression profile of lipid metabolism-related differentially expressed genes with each phenotype. Variables were standardized before Euclidean distance matrices were constructed. Pearson correlations between the upper-triangular elements of the distance matrices were used as the Mantel statistic, and significance was assessed with 9999 permutations.

2.11. LMH Cell Culture and Palmitic/Oleic Acid Treatment

LMH cells from the laboratory's cryopreserved stock were cultured in DMEM/F12 medium (319-087 CL; Wisent Inc., Saint-Jean-Baptiste, QC, Canada), which contains 365.10 mg/L L-glutamine in its basal formulation, supplemented with 10% fetal bovine serum (TransGen Biotech, Beijing, China) and 1% penicillin–streptomycin solution (TransGen Biotech, Beijing, China) at 37 °C in 5% CO2. The complete medium was passed through a 0.22 μm filter, stored at 4 °C, and used within 2 wk.

At approximately 50% confluence, cells were pretreated with 5-ALA for 24 h. The medium was then replaced with fresh medium containing both 5-ALA and a mixture of 100 μmol/L palmitic acid and 200 μmol/L oleic acid for a further 12 h. The principal experiments used 500 μmol/L 5-ALA; 250 and 500 μmol/L were compared in the dose-screening experiment. Control and PA/OA-only conditions were included. The four groups used in the HMOX1-silencing experiment are specified in Section 2.16. "FFA" denotes combined treatment with 100 μmol/L PA and 200 μmol/L OA.

2.12. Cell Viability

LMH cells were seeded in 96-well plates with 100 μL of cell suspension per well and treated for 24 h with 0, 100, 250, 500, or 1000 μmol/L 5-ALA. CCK-8 reagent (10 μL; Beyotime Biotechnology, Shanghai, China) was added to each well, and the plates were incubated for an additional 2 h. Absorbance at 450 nm was measured using a Synergy 2 multimode microplate reader (BioTek Instruments, Inc., Winooski, VT, USA), and viability was expressed relative to the untreated control, which was set to 100%.

2.13. Cellular Lipid Accumulation

Cellular TG was measured using an enzymatic tissue/cell TG kit (Applygen Technologies). After treatment, cells were collected and lysed, and the lysate was centrifuged at 000× g for 10 min at 4 °C. TG in the supernatant was normalized to total protein.

For Oil Red O staining, cells were fixed in 4% paraformaldehyde for 30 min. A working solution was prepared by mixing the Oil Red O stock solution and deionized water at 3:2, allowing the mixture to stand for 10 min, and filtering it through a 0.22 μm membrane. Cells were stained for 15 to 20 min in the dark, briefly differentiated with 60% isopropanol for 3 to 5 s, counterstained with hematoxylin for 1 to 2 min, and imaged via light microscopy. The cell-specific Oil Red O staining kit was obtained from Beijing Solarbio Science & Technology Co., Ltd. (Beijing, China).

Neutral lipid droplets were also detected with BODIPY 493/503 (Beyotime Biotechnology). Fluorescence emission was collected in the 505 to 550 nm range after 488 nm

excitation, and the geometric mean fluorescence intensity was used for quantification. Nuclei were counterstained with Hoechst 33342 for fluorescence imaging. Images were acquired using a Leica TCS SP8 confocal laser-scanning microscope (Leica Microsystems, Wetzlar, Germany) under identical settings.

2.14. Cellular Redox and ATP Measurements

Cellular SOD activity and MDA content were measured using commercial kits, respectively (Nanjing Jiancheng Bioengineering Institute), and normalized to total protein. ATP was measured with a luciferase-based assay kit (Beyotime Biotechnology). Cells were lysed in 200 μL of precooled ATP lysis buffer on ice for 10 min, and lysates were centrifuged at 12,000× *g* for 5 min at 4 °C. The ATP detection reagent was reconstituted and diluted 1:9 with assay diluent and then equilibrated for approximately 30 min at room temperature in the dark. Standards ranging from 0.01 to 10 μmol/L were prepared. The detection reagent (100 μL) and sample or standard (20 μL) were combined in an opaque 96-well plate, and luminescence was recorded immediately with a 10 s integration time. ATP content was calculated from the standard curve and normalized to total protein.

2.15. Cellular Reactive Oxygen Species and Mitochondrial Membrane Potential

Intracellular reactive oxygen species (ROS) were measured with CellROX Green reagent (5 μmol/L; Invitrogen, Carlsbad, CA, USA). After treatment, cells were detached using 0.25% EDTA-free trypsin, washed with phosphate-buffered saline, incubated with CellROX Green in serum-free medium for 30 min at 37 °C in the dark, washed again, and analyzed in the FITC channel on a BD FACSVerse flow cytometer (BD Biosciences, San Jose, CA, USA). At least 10,000 cells were acquired per sample, and the mean fluorescence intensity was analyzed with FlowJo 10.8.1 (BD Life Sciences, Ashland, OR, USA).

Mitochondrial membrane potential was assessed using the JC-1 kit (Beyotime Biotechnology). JC-1 monomers were detected in the FITC channel and aggregates in the PE channel after 488 nm excitation. The aggregate-to-monomer fluorescence ratio was used as the index of mitochondrial membrane potential. Parallel fluorescence images were acquired after Hoechst 33342 counterstaining using the Leica TCS SP8 microscope under consistent acquisition settings.

2.16. HMOX1 Silencing

LMH cells were grown in 48-well or 6-well plates to approximately 50% confluence. Cells were transfected with a chicken HMOX1-targeting siRNA (siHMOX1) or a non-targeting negative-control siRNA (siNC) at a final concentration of 50 nmol/L using jetPRIME reagent (Polyplus Transfection, Illkirch, France). Both siRNAs were obtained from Tsingke Biotechnology Co., Ltd. (Nanjing, Jiangsu, China). After 12 h of transfection, cells underwent 5-ALA pretreatment and PA/OA exposure as described above. Silencing efficiency was verified via RT-qPCR and Western blotting. The siHMOX1 sense sequence was 5′-CACAAGGAGUGUUAACAAA-dTdT-3′, and the antisense/guide sequence was 5′-UUUGUUAACACUCCUUGUG-dTdT-3′. The functional experiment comprised four groups: CON, FFA, FFA + 5-ALA + siNC, and FFA + 5-ALA + siHMOX1. Following transfection, the 5-ALA groups were pretreated with 500 μmol/L 5-ALA for 24 h; the medium was then replaced with fresh medium containing 500 μmol/L 5-ALA, 100 μmol/L PA, and 200 μmol/L OA for 12 h.

2.17. Statistical Analysis

Data are presented as the mean ± SEM. Normality and homogeneity of variance were assessed using the Shapiro–Wilk and Levene's tests, respectively. Two-group comparisons between the CON and 5-ALA groups were analyzed using Student's t-test or the

Mann–Whitney U-test, as appropriate. For LMH-cell experiments without HMOX1 silencing that involved multiple groups, one-way ANOVA followed by Tukey's HSD test was applied. The silencing experiment used the treatment group as the analysis factor across CON, FFA, FFA + 5-ALA + siNC, and FFA + 5-ALA + siHMOX1, with emphasis on the comparison between the two siRNA conditions under the same FFA + 5-ALA exposure. For in vivo measurements, the replicate cage was considered the experimental unit (n = 6 per treatment). Cell experiments were independently repeated three times (n = 3), with each independent biological replicate serving as the experimental unit. Differences were considered statistically significant at $p < 0.05$. Statistical analyses were performed using IBM SPSS Statistics 26.0 (IBM Corp., Armonk, NY, USA) and GraphPad Prism 9.0 (GraphPad Software, San Diego, CA, USA).

3. Results

3.1. Network Pharmacology Analysis Identified Candidate Targets of 5-ALA Associated with Hepatic Lipid Metabolism and Redox Homeostasis

The intersection of fatty-liver-associated genes with 5-ALA-associated candidates yielded 155 source-level symbols, which were standardized to 157 human reference genes (Figure 1A). The STRING 12.0 functional-association network contained 129 connected nodes and 338 edges (Figure 1B). HMOX1, CPT1A, CPT2, SIRT1, HMGCR, NFE2L2, and MAPK family members were represented in the network; selected genes were highlighted because of their relevance to redox regulation and lipid metabolism. Functional enrichment linked the candidates to oxidative-stress responses, ROS metabolism, cellular redox homeostasis, lipid metabolism, fatty acid transport, cholesterol metabolism, apoptosis, and inflammatory responses (Figure 1D,F).

Selected significant KEGG terms included lipid and atherosclerosis, metabolic pathways, apoptosis, TNF signaling, sphingolipid signaling, and arachidonic acid metabolism (Figure 1C,E). The 139 chicken orthologs also showed the significant enrichment of lipid metabolism, responses to oxidative stress, and antioxidant activity against the chicken annotation background (Table S8). These analyses generated hypotheses concerning lipid metabolism and redox regulation for evaluation alongside the animal and cell experiments.

3.2. Dietary 5-ALA Supplementation Attenuates Hepatic Lipid Deposition and Enhances Antioxidant Capacity in Laying Hens

The representative gross liver appearance at the end of the trial is shown in Figure 2B. Neither the absolute liver weight nor liver index differed between dietary treatments (Figure 2C,D). Hepatic TG, TC, and FC were all lower in 5-ALA-fed hens than in control-fed hens, whereas CE was unchanged (Figure 2E,F). Histological scoring returned lower steatosis and lobular inflammation scores after 5-ALA supplementation, and the H&E and Oil Red O images consistently showed reduced steatosis, less inflammatory infiltration, and fewer lipid droplets (Figure 2G,H).

Serum biochemistry showed that 5-ALA supplementation lowered AST activity and the AST/ALT ratio, while ALT activity was unaffected (Figure 2I–K). Serum TG and TC concentrations were also lower in 5-ALA-fed hens than in control-fed hens (Figure 2L,M). Hepatic SOD activity was higher and hepatic MDA was lower in 5-ALA-fed hens (Figure 2N,O). Collectively, these findings indicate that dietary 5-ALA supplementation attenuates hepatic lipid deposition and improves the hepatic histomorphology and antioxidant status in laying hens.

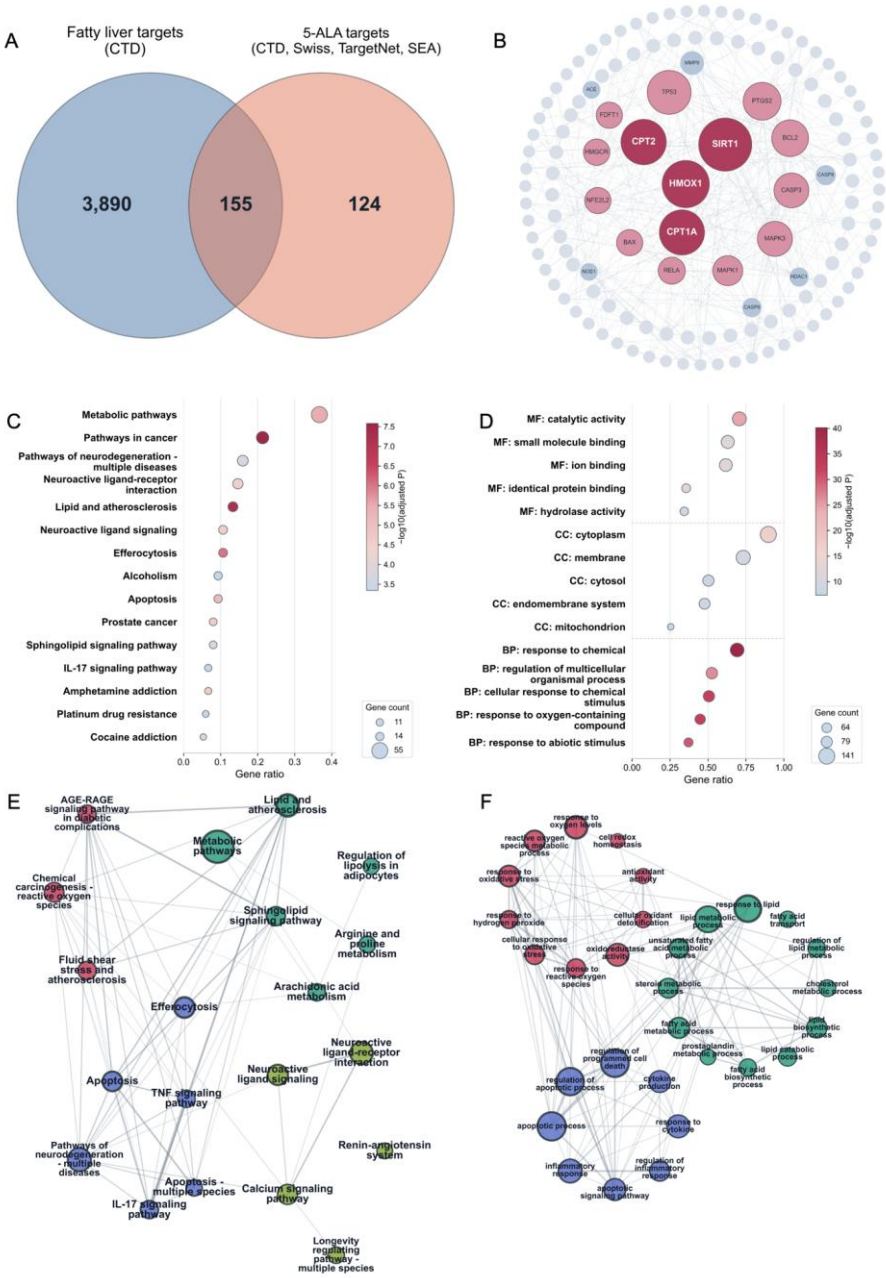

Figure 1. Cross-species candidate collection and human reference-network analysis of 5-ALA and fatty liver. (**A**) Intersection of 4045 CTD fatty-liver-associated symbols and 279 5-ALA-associated source symbols, yielding 155 candidates. Identifier standardization produced 157 human reference genes. (**B**) STRING 12.0 functional-association network of the human reference genes (combined score ≥ 0.700; 129 connected nodes and 338 edges). Larger, colored nodes highlight genes selected for discussion. (**C**) Selected significant KEGG pathways. (**D**) Selected significant GO molecular function (MF), cellular component (CC), and biological process (BP) terms. The bubble size indicates the gene count, and color indicates −log10(g:SCS-adjusted *p*); gene ratio is the fraction of the annotated query genes represented in a term. (**E**) Selected KEGG enrichment network. (**F**) Selected GO enrichment network, including BP and MF terms. In (**E**,**F**), node size represents the gene count, border width reflects the enrichment significance, colors indicate the displayed functional groups, and edges indicate shared genes. All displayed enriched terms meet g:SCS-adjusted $p < 0.05$. The 139 chicken orthologs and chicken-background enrichment results are provided in Tables S4 and S8.

The mean whole-blood hemoglobin concentration was 144.51 ± 4.36 g/L in the CON group and 175.21 ± 5.13 g/L in the 5-ALA group (mean ± SEM; six matched birds per treatment). Group means ± SEM are provided in Table S1.

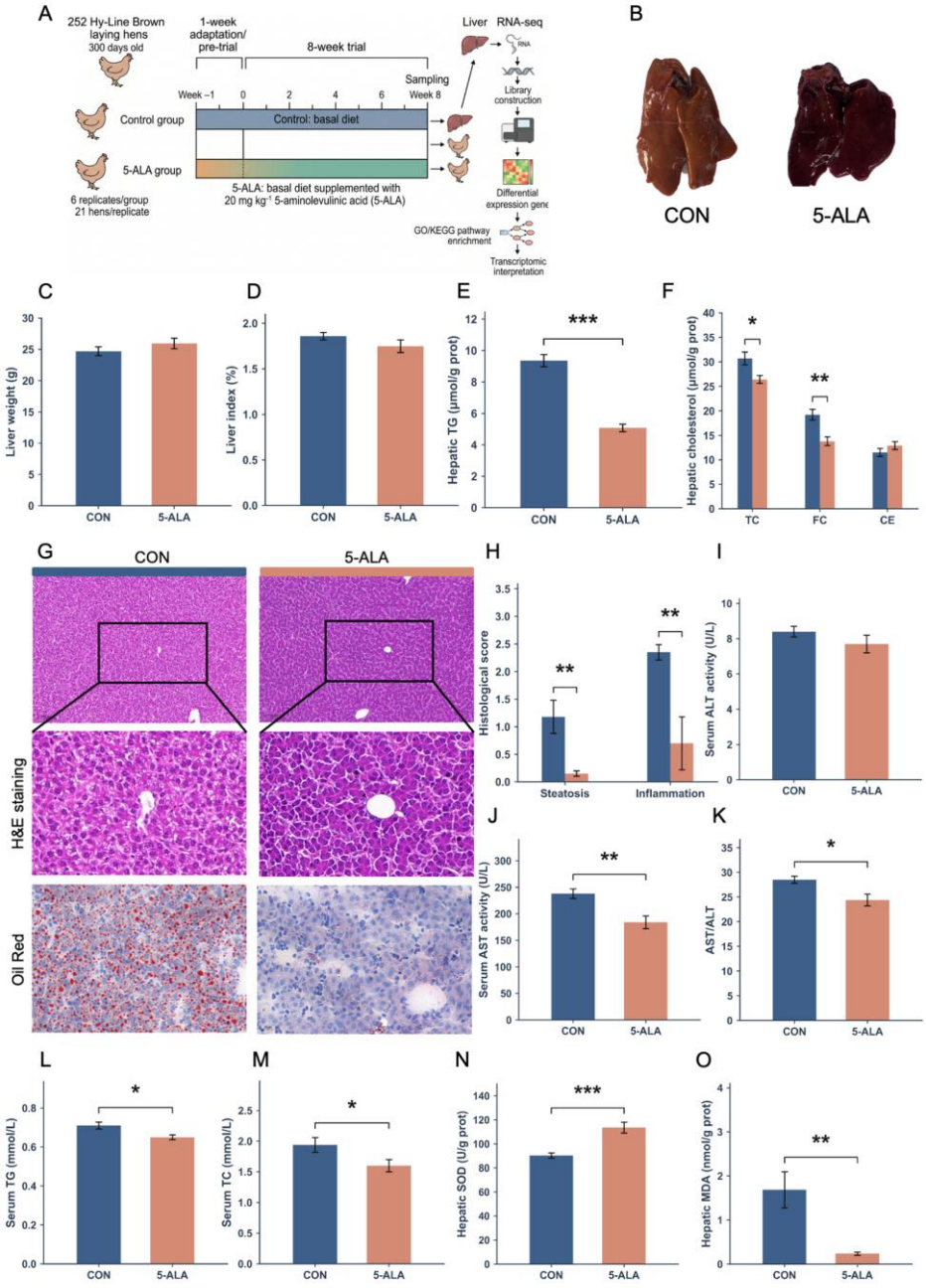

Figure 2. Effects of dietary 5-ALA on hepatic lipid deposition, histology, and redox-related indices in laying hens. (**A**) Animal experimental design and transcriptomic-analysis workflow. (**B**) Representative gross liver appearance. (**C**) Liver weight. (**D**) Liver index. (**E**) Hepatic TG content. (**F**) Hepatic TC, FC, and CE contents. (**G**) Representative H&E- and Oil Red O-stained images. (**H**) Hepatic steatosis and lobular inflammation scores. (**I**) Serum ALT activity. (**J**) Serum AST activity. (**K**) AST/ALT ratio. (**L**) Serum TG content. (**M**) Serum TC content. (**N**) Hepatic SOD activity. (**O**) Hepatic MDA content. CON, control group; 5-ALA, basal diet supplemented with 20 mg/kg 5-ALA. The cage was the experimental unit in the animal experiment, with six replicates per treatment. Bar-chart data are presented as means ± SEM. * $p < 0.05$, ** $p < 0.01$, *** $p < 0.001$.

3.3. Dietary 5-ALA Supplementation Reshapes the Hepatic Transcriptomic Profile in Laying Hens

The sample-to-sample correlation revealed high overall similarity across the 12 liver transcriptomes (Figure 3A). Two-dimensional principal component analysis showed partially overlapping distributions of the two dietary groups; PC1 and PC2 explained 21.65% and 17.57% of the variance, respectively (Figure 3B). Applying $|\log_2 \text{fold change}| \geq 1$ and $p < 0.05$, 301 differentially expressed genes were identified, 124 up-regulated and 177 down-regulated in 5-ALA-fed hens (Figure 3C,D). The heatmap revealed clearly distinct expression patterns between the two treatments (Figure 3E). Among the representative transcripts shown in Figure 3F, HKDC1, HSP90B1, CRELD2, DHCR24, HMGCR, CYP51A1, and PER2 were significantly down-regulated in the 5-ALA-supplemented group, whereas ACAA1, SLC22A5, ACSL1, PEX11A, PPARGC1A, CPT1A, and HMGCL were significantly up-regulated.

Eight chicken ortholog candidates overlapped with the 301 differentially expressed genes: CPT1A, CYP1A1, CYP1A2, FDFT1, FDPS, HMGCR, MMP1, and PLIN1. Their identifiers and expression statistics are listed in Table S2; the RNA-seq results and candidate sources for HMOX1 and CPT1A are reported separately in Table S3.

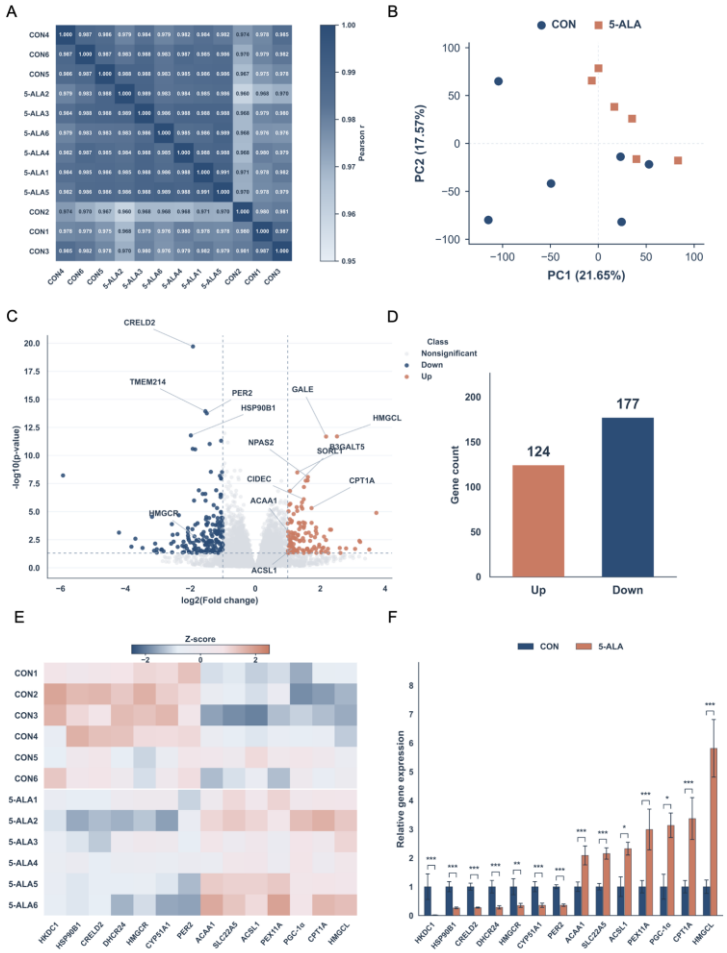

Figure 3. Hepatic transcriptomic expression profiles in laying hens after dietary 5-ALA supplementation. (**A**) Pearson correlation heatmap of the 12 liver samples. (**B**) Two-dimensional principal component analysis of the 12 samples, with each point representing one liver sample; PC1 and PC2 explained 21.65% and 17.57% of the variance, respectively. (**C**) Volcano plot generated using $p < 0.05$

and |log2FC| ≥ 1 as the thresholds. (**D**) Numbers of differentially expressed genes, including 124 up-regulated and 177 down-regulated genes. (**E**) Heatmap of Z-score-normalized expression of selected differentially expressed genes across the 12 liver samples. (**F**) Relative expression of selected differentially expressed genes between groups. Six biological samples were analyzed per treatment; data are presented as means ± SEM. * $p < 0.05$, ** $p < 0.01$, *** $p < 0.001$.

3.4. Transcriptomic Analyses Revealed Enrichment of Fatty Acid Degradation, Peroxisome, and Cholesterol Biosynthesis Pathways

KEGG enrichment analysis assigned the differentially expressed genes chiefly to steroid biosynthesis, PPAR signaling, protein processing in the endoplasmic reticulum, adipocytokine signaling, glycosphingolipid biosynthesis, terpenoid backbone biosynthesis, phagosome, and glycolysis/gluconeogenesis (Figure 4A). GO biological-process analysis further implicated cholesterol and steroid biosynthesis, the endoplasmic-reticulum unfolded protein response, regulation of bile acid biosynthesis, regulation of circadian rhythm, proline biosynthesis, and cellular responses to ammonium ions (Figure 4B).

GSEA revealed positive enrichment towards 5-ALA-fed hens of fatty acid degradation (NES = 1.73, $p = 0.005$, FDR = 0.033), peroxisome (NES = 1.83, $p < 0.001$, FDR = 0.020) and PPAR signaling (NES = 1.59, $p = 0.016$, FDR = 0.094), whereas terpenoid backbone biosynthesis was enriched towards control-fed hens (NES = −1.93, $p < 0.001$, FDR = 0.008; Figure 4C–F). Collectively, these findings indicate that dietary 5-ALA supplementation was associated with coordinated transcriptomic changes in fatty acid degradation, peroxisome-related, and lipid-metabolism-related pathways in laying hens.

3.5. Dietary 5-ALA Supplementation Increases Hepatic HO-1 and Fatty-Acid-Metabolism- and Mitochondrial Function-Related Genes and Proteins in Laying Hens

Within the lipid metabolism-related interaction network, ACAA1, CPT1A, ACSL1, and PGC-1α emerged as highly connected nodes, linked to HMGCL, HMGCR, CPT2, ACOX1, members of the PEX family and additional lipid-metabolic molecules (Figure 5A). RT-qPCR showed higher hepatic expression of *CPT1A*, *HMOX1*, *ACAA1*, *ACSL1*, *PPARGC1A*, *TFAM*, *TOMM20*, and *SDHB* after 5-ALA supplementation (Figure 5B), and immunoblotting with matched densitometry confirmed parallel increases in HO-1, CPT1A, ACAA1, ACSL1, PGC-1α, TFAM, TOM20, and SDHB proteins (Figure 5C,D).

Spearman correlation analysis revealed significant positive and negative associations linking *HMOX1*, lipid-metabolic differentially expressed genes, and phenotypic variables including hemoglobin, hepatic TG, MDA, SOD, and FC (Figure 5E). Mantel testing further showed that both *HMOX1* expression and the overall expression profile of the lipid-metabolic gene set were associated with selected phenotypic indices (Figure 5F). Together, these findings show associations among HMOX1 expression, hepatic lipid deposition, oxidative-status indices, and the fatty-acid-metabolism-related gene set.

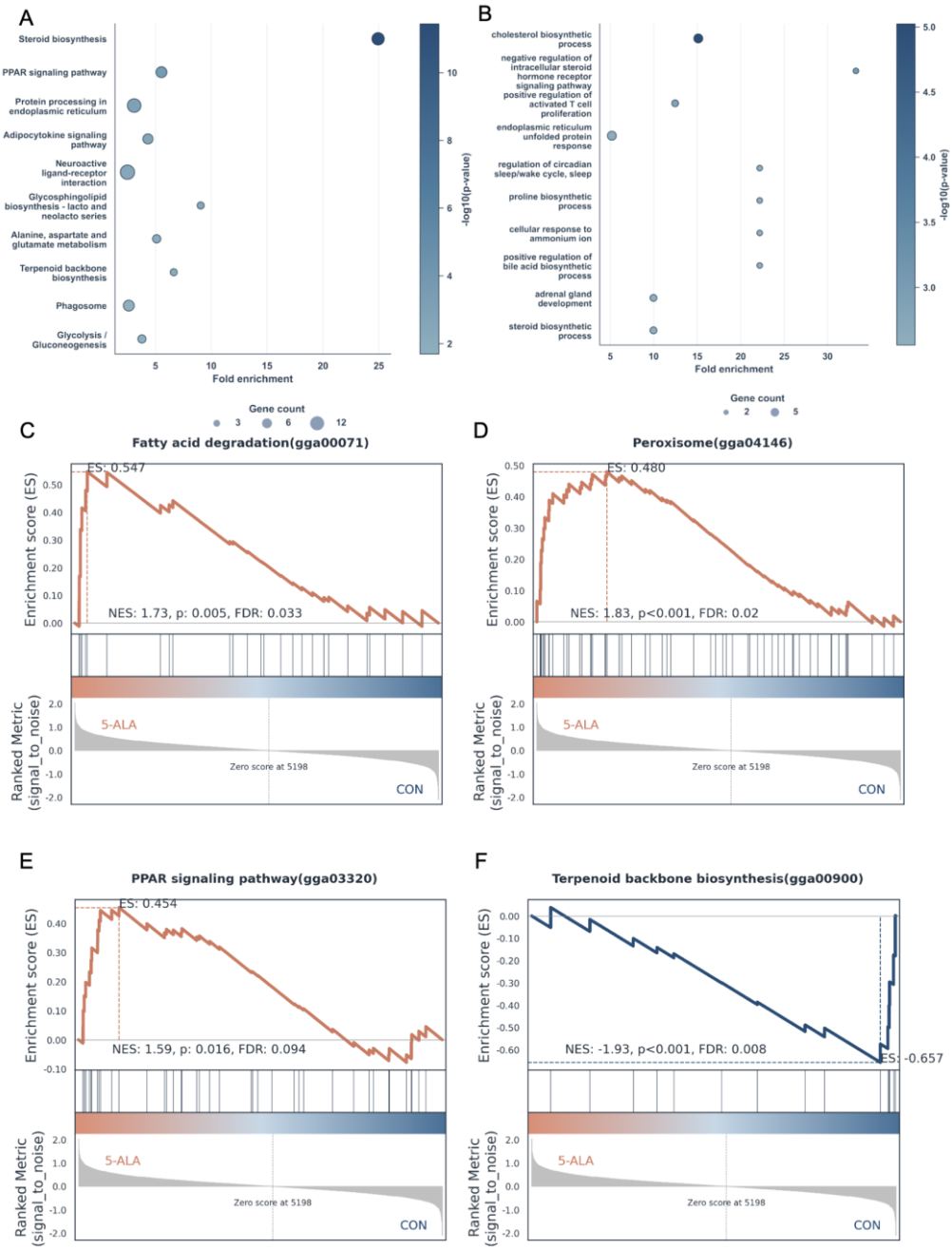

Figure 4. Functional enrichment and gene set enrichment analyses of differentially expressed genes. (**A**) KEGG pathway enrichment analysis. (**B**) GO biological-process enrichment analysis. (**C–F**) GSEA curves for fatty acid degradation, peroxisome, PPAR signaling, and terpenoid backbone biosynthesis. A positive NES indicates enrichment in the 5-ALA group, whereas a negative NES indicates enrichment in the CON group; the NES, *p* value, and FDR are shown within each panel.

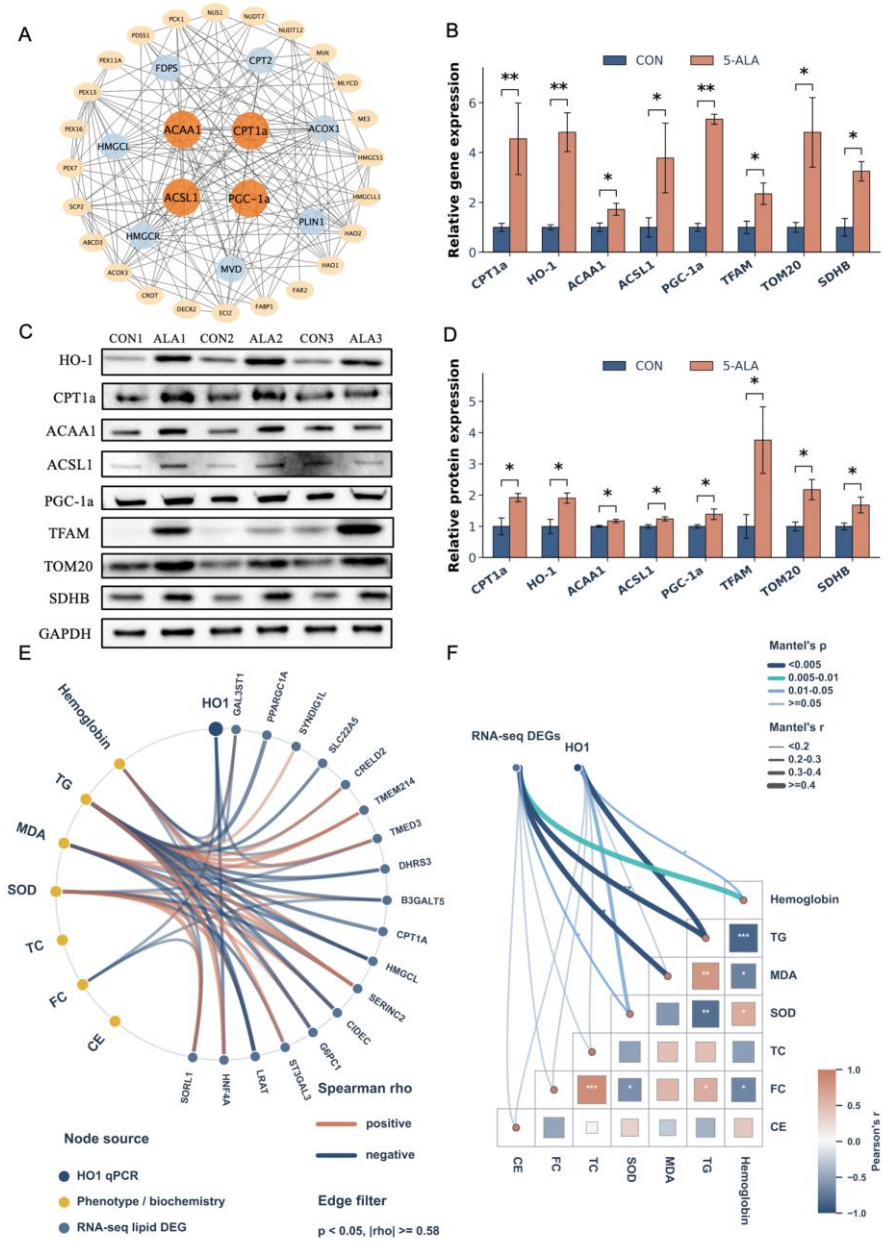

Figure 5. Hepatic HO-1 and markers of fatty acid metabolism and mitochondrial function after 5-ALA supplementation. (**A**) Protein-interaction network related to lipid metabolism. (**B**) RT-qPCR results for CPT1A, HMOX1, ACAA1, ACSL1, PPARGC1A, TFAM, TOMM20, and SDHB, with six biological samples per treatment. (**C**) Representative Western blot bands for HO-1, CPT1A, ACAA1, ACSL1, PGC-1α, TFAM, TOM20, and SDHB. (**D**) Densitometric quantification of Western blots. (**E**) Spearman correlation network of HMOX1, phenotypic indices, and lipid-metabolism-related candidate genes; displayed edges met two-sided $p < 0.05$ and $|\varrho| \geq 0.58$, with gene and edge selection as described in Section 2.10, and edge color represents the direction of the correlation. (**F**) Mantel analysis of HMOX1 or the overall expression profile of lipid-metabolism-related candidate genes with phenotypic indices, together with a Pearson correlation matrix of the phenotypic indices. Correlation analyses pooled 12 matched individual samples (six CON and six 5-ALA), with HMOX1 measured via RT-qPCR in all 12 birds and gene expression and phenotypes matched within the bird. * $p < 0.05$, ** $p < 0.01$, *** $p < 0.001$.

3.6. 5-ALA Alleviates PA/OA-Induced Lipid Accumulation, Oxidative Stress, and Mitochondrial Dysfunction in LMH Cells

Cell viability remained close to that of untreated cells across 5-ALA concentrations from 100 to 1000 μmol/L (Figure 6A). Following 24 h of 5-ALA pretreatment, cells were exposed, for 12 h, to PA/OA in fresh medium that also contained 5-ALA. The PA/OA challenge increased cellular TG, and this 5-ALA treatment regimen attenuated the rise, with a stronger effect at 500 μmol/L than at 250 μmol/L (Figure 6B). Oil Red O staining and BODIPY 493/503 fluorescence consistently showed that PA/OA promoted intracellular lipid-droplet accumulation and that 500 μmol/L 5-ALA blunted this response (Figure 6E). Relative to untreated cells, PA/OA challenge lowered SOD activity, the ATP content, and the JC-1 aggregate-to-monomer ratio and raised MDA and ROS fluorescence. 5-ALA treatment reversed these changes, restoring SOD activity, the ATP content, and mitochondrial membrane potential and lowering MDA and ROS (Figure 6C,D,G–I). JC-1 fluorescence images and ROS flow-cytometry histograms mirrored the quantitative data (Figure 6F,I). Immunoblotting showed that 5-ALA raised the abundance of HO-1, CPT1A, ACAA1, ACSL1, PGC-1α, TFAM, COXIV, and MFN2 above the PA/OA-only condition (Figure 6J,K). Overall, 5-ALA attenuated PA/OA-induced lipid accumulation and oxidative stress and restored the ATP content and mitochondrial membrane potential, accompanied by increased abundance of proteins related to fatty acid metabolism and mitochondrial function in LMH cells.

3.7. HMOX1 Silencing Attenuates Several Cytoprotective Responses to 5-ALA in PA/OA-Challenged LMH Cells

In the PA/OA-loaded LMH model, 5-ALA increased HMOX1 mRNA and HO-1 protein, and siHMOX1 lowered both, confirming effective silencing (Figure 7A). PA/OA challenge raised cellular TG, BODIPY fluorescence, and Oil Red O staining, and 24 h 5-ALA pretreatment followed by continued 5-ALA exposure during the 12 h PA/OA challenge attenuated these lipid-accumulation indices. After HMOX1 silencing, cellular TG, BODIPY fluorescence, and Oil Red O staining were all higher than in siNC-transfected cells that had received 5-ALA (Figure 7B–D).

PA/OA challenge lowered the JC-1 aggregate-to-monomer ratio, SOD activity, and ATP content and raised MDA and ROS, and 5-ALA reversed all these changes. Relative to siNC-transfected cells receiving 5-ALA, *HMOX1* silencing lowered the JC-1 aggregate-to-monomer ratio, SOD activity, and ATP content and raised MDA and ROS (Figure 7E–K). JC-1 imaging and ROS flow-cytometry histograms were consistent with the quantitative results (Figure 7E,F,J,K).

Immunoblotting showed that 5-ALA raised CPT1A, ACAA1, PGC-1α, TFAM, and TOM20 above the PA/OA-only condition. After HMOX1 silencing, ACAA1 protein fell significantly below the 5-ALA + siNC condition, while CPT1A, PGC-1α, TFAM, and TOM20 showed numerical decreases that did not reach statistical significance (Figure 7L,M). Collectively, HMOX1 silencing increased intracellular lipid accumulation and oxidative stress and reduced the ATP content and mitochondrial membrane potential, supporting a contribution of HO-1 to the cytoprotective effects of 5-ALA in LMH cells.

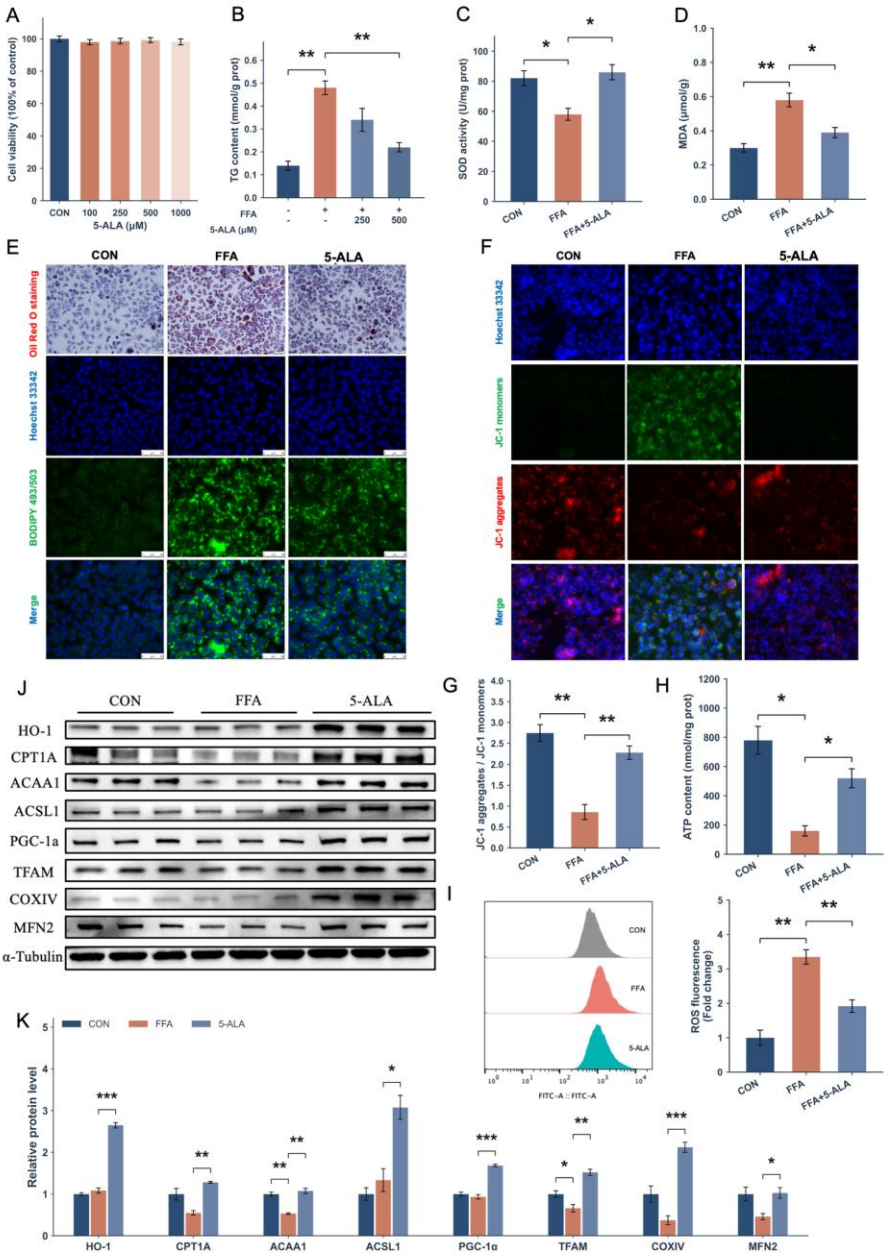

Figure 6. 5-ALA effects on lipid, redox, and mitochondrial indices in PA/OA-treated LMH cells. (**A**) Cell viability after treatment with different concentrations of 5-ALA. (**B**) Effects of different 5-ALA concentrations on PA/OA-induced cellular TG accumulation. (**C**) SOD activity. (**D**) MDA content. (**E**) Oil Red O staining, Hoechst 33342 nuclear staining, BODIPY 493/503 fluorescence images, and merged images of lipid droplets. (**F**) JC-1 fluorescence images. (**G**) JC-1 aggregate-to-monomer ratio. (**H**) ATP content. (**I**) ROS flow-cytometry distributions and corresponding fluorescence quantification. (**J**) Representative Western blot bands for HO-1, CPT1A, ACAA1, ACSL1, PGC-1α, TFAM, COXIV, and MFN2. (**K**) Densitometric quantification of Western blots. "FFA" denotes combined treatment with 100 μmol/L PA and 200 μmol/L OA; the 5-ALA concentration used in the principal experiments was 500 μmol/L. In (**B**–**K**), cells were pretreated with 5-ALA for 24 h, followed by replacement with fresh medium containing both 5-ALA and PA/OA for a further 12 h. Data are presented as means ± SEM. * $p < 0.05$, ** $p < 0.01$, *** $p < 0.001$.

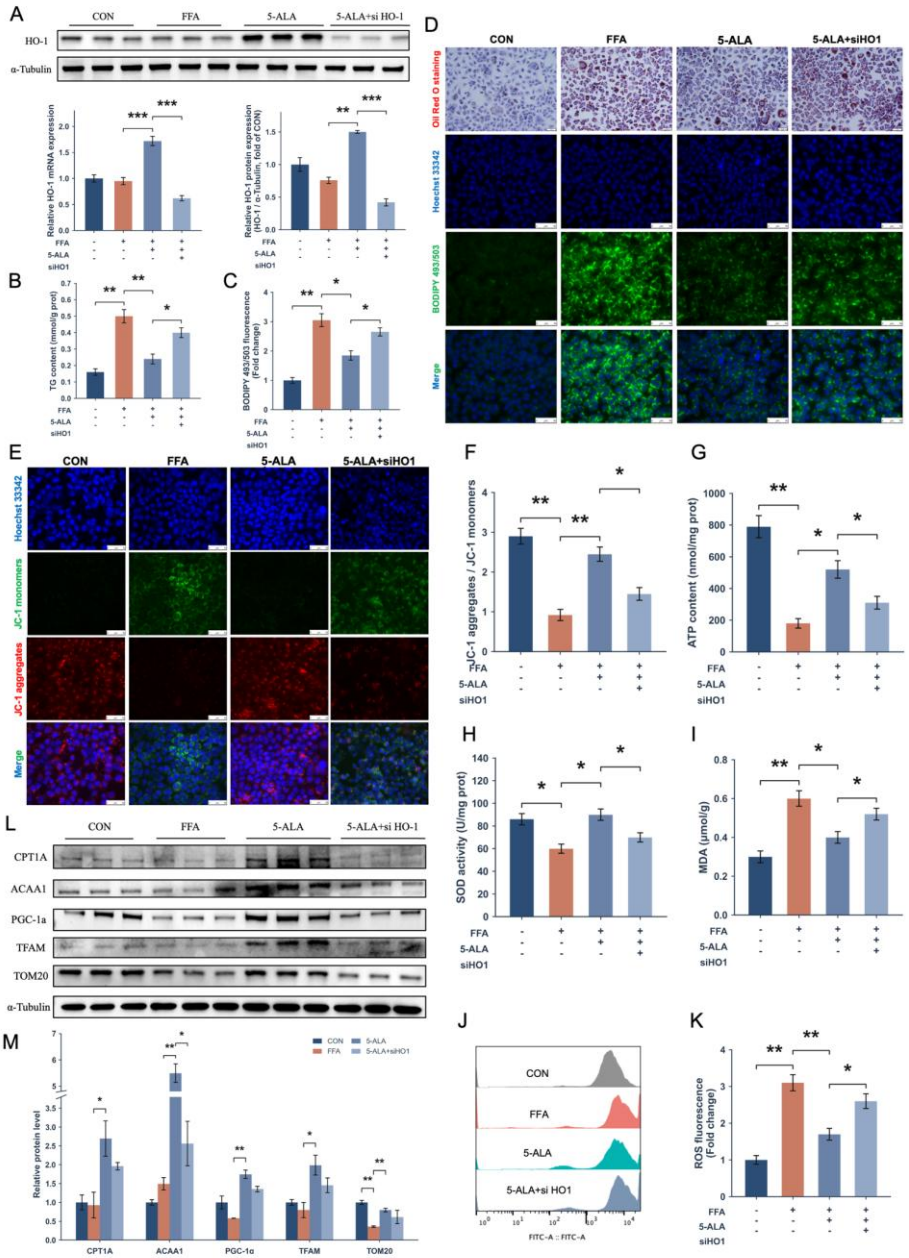

Figure 7. Effects of HMOX1 silencing on 5-ALA responses in PA/OA-treated LMH cells. (**A**) HMOX1 mRNA, HO-1 protein, and representative Western blot bands. (**B**) Cellular TG content. (**C**) BODIPY 493/503 fluorescence quantification. (**D**) Oil Red O staining, Hoechst 33342 nuclear staining, BODIPY 493/503 fluorescence images, and merged images. (**E**,**F**) JC-1 fluorescence images and aggregate-to-monomer ratio. (**G**) ATP content. (**H**) SOD activity. (**I**) MDA content. (**J**,**K**) ROS flow-cytometry distributions and fluorescence quantification. (**L**,**M**) Western blotting and densitometric quantification of CPT1A, ACAA1, PGC-1α, TFAM, and TOM20. "FFA" denotes combined treatment with 100 μmol/L PA and 200 μmol/L OA. "siHO1" in the figure denotes the HMOX1-targeting siRNA (siHMOX1). The four groups were CON, FFA, FFA + 5-ALA + siNC, and FFA + 5-ALA + siHMOX1. After transfection, the third and fourth groups received 500 μmol/L 5-ALA for 24 h, followed by replacement with fresh medium containing 500 μmol/L 5-ALA and PA/OA for 12 h. Data are presented as means ± SEM. * $p < 0.05$, ** $p < 0.01$, *** $p < 0.001$.

4. Discussion

Dietary 5-ALA lowered hepatic lipid deposition and improved redox-related indices in laying hens, with parallel changes in transcripts and proteins associated with fatty acid metabolism, peroxisomes, and mitochondria. In PA/OA-loaded LMH cells, 5-ALA likewise reduced lipid accumulation and oxidative stress while restoring the ATP content and mitochondrial membrane potential. After *HMOX1* silencing, TG and lipid-droplet accumulation, ROS, and MDA all rose, whereas SOD activity, the ATP content, and mitochondrial membrane potential fell, relative to siNC-transfected cells receiving 5-ALA. Together, these observations indicate that HO-1 participates in the hepatocellular response to 5-ALA.

Dietary 5-ALA lowered hepatic TG, TC, and FC and reduced steatosis, inflammation, and lipid-droplet deposition, indicating improved hepatic lipid homeostasis under normal laying conditions. Network analysis flagged lipid metabolism and redox regulation as candidate processes, and, across the in vivo and cellular experiments, elevated HO-1 expression coincided with coordinated changes in fatty-acid-metabolic, peroxisomal, and mitochondrial genes and proteins. Previous poultry studies evaluated 5-ALA principally in the context of iron status, hematology, and stress responses. In laying hens, doses of 5, 10, and 15 mg/kg and combinations of 5 or 10 mg/kg 5-ALA with vitamin C have been tested [20,21]. The 20 mg/kg dose used here was associated with a higher mean whole-blood hemoglobin concentration (Table S1) and lower indices of hepatic lipid deposition and oxidative stress. Consistent with the present findings, 5-ALA supplementation increased hepatic HO-1 expression in lipopolysaccharide-challenged broilers [12] and renal HO-1 mRNA in heat-stressed laying hens [13]. Outside poultry, 5-ALA lowered the hepatic lipid content and increased AMPK phosphorylation in high-fat-diet-fed mice, and complementary HepG2 experiments reported higher PGC-1α and CPT1A expression [10]. The present study extends these findings by demonstrating that 5-ALA also reshapes hepatic lipid metabolism in the highly lipogenic liver of the laying hens.

The redox effects of 5-ALA may depend on the exposure level and cellular context. Menezes et al. found that ALA treatment increased lipid peroxidation and was accompanied by increased p53 and decreased Bcl-2 expression in primary rat hepatocytes [22]. These findings suggest that ALA accumulation and oxidation can increase the oxidative burden and alter apoptosis-related regulation. In the present study, MDA and ROS decreased under the treatment conditions examined. The contrasting findings raise the possibility of a biphasic response influenced by the dose and cell model. Further dose-comparison studies should assess both protective effects and oxidative injury to establish an effective dose range and its safety margins.

KEGG and GO analyses identified lipid-metabolism-related processes, and GSEA showed positive enrichment of the fatty acid degradation and peroxisome gene sets in 5-ALA-fed hens. The parallel increases in *CPT1A*, *ACAA1*, and *ACSL1* at both the mRNA and protein levels are consistent with the observed reduction in hepatic lipid deposition. Late-phase laying hens fed a low-energy, low-protein diet showed hepatic fat accumulation and lower expression of the β-oxidation genes ACOX1, HADHA, EHHADH, and ACAA1 than hens fed a normal-energy, normal-protein diet [23]. CPT1A governs the rate-limiting entry of long-chain fatty acyl groups into mitochondrial β-oxidation via the carnitine shuttle [24], while ACAA1 catalyzes the thiolytic step of peroxisomal β-oxidation [25]. ACSL1 generates long-chain acyl-CoA for both fatty acid oxidation and glycerolipid synthesis, linking fatty acid activation to both pathways [26]. 5-ALA also increased PGC-1α, TFAM, and TOM20, which are involved in mitochondrial transcriptional regulation, mtDNA organization, and outer-membrane protein import, respectively [3,27]. SDHB, an iron–sulfur subunit of respiratory complex II, was also increased. Other dietary interventions have also reduced hepatic lipid accumulation in laying hens [28–30]. In Jinhua pigs,

10% fermented broccoli stem and leaf feed reduced the backfat thickness and increased *CPT1A* mRNA in dorsal subcutaneous fat [31].

Dietary 5-ALA also altered hepatic cholesterol homeostasis. Hepatic TC and FC declined, whereas CE was unchanged. Several cholesterol biosynthesis transcripts, including *HMGCR*, were down-regulated, and terpenoid backbone biosynthesis was enriched towards control-fed hens. In other words, 5-ALA was associated with lower expression of cholesterol biosynthesis genes and lower hepatic FC, without a compensatory shift in CE. Excess free cholesterol within mitochondria can perturb membrane properties, deplete mitochondrial glutathione, promote ROS generation, and disrupt respiratory supercomplex assembly [32]. The reduction in hepatic FC, together with lower TG deposition, may therefore have contributed to the increase in SOD activity and decrease in MDA content that followed 5-ALA supplementation [32].

The PA/OA challenge in LMH cells provided a tractable hepatocellular model in which to interrogate the response to 5-ALA. Palmitic acid is strongly lipotoxic, whereas oleic acid is more readily channeled into TG and stored within lipid droplets; together, the two fatty acids elicit both lipid accumulation and cellular stress [33,34]. Lipid droplets not only serve as intracellular lipid stores but can also transiently sequester fatty acids that would otherwise drive lipotoxicity [33,34]. A comparable PA/OA challenge in laying-hen hepatocytes increased lipid droplets, TG, ROS, and MDA and lowered SOD activity and mitochondrial membrane potential [35]. Here, 5-ALA reduced TG, lipid staining, ROS, and MDA and raised SOD activity, the ATP content, and mitochondrial membrane potential. It also up-regulated CPT1A, ACAA1, PGC-1α, TFAM, COXIV, and MFN2 in these cells, mirroring the in vivo hepatic findings.

5-ALA increased HO-1 expression in both the laying-hen liver and PA/OA-treated LMH cells. After HMOX1 silencing, cellular TG and lipid-droplet accumulation, ROS and MDA rose, and SOD activity, the ATP content, and mitochondrial membrane potential fell. The directionality of these changes is consistent with a contribution of HO-1 to the cellular effects of 5-ALA. Among the proteins examined, ACAA1 decreased significantly after HMOX1 silencing, whereas CPT1A, PGC-1α, TFAM, and TOM20 showed numerical decreases without statistical significance. The protein results therefore indicate the attenuation of selected responses. Hashimoto et al. [11] similarly reported that 5-ALA induced HO-1 and attenuated endoplasmic reticulum stress and lipotoxic apoptosis in palmitate-treated Huh7 cells; because NRF2 mRNA did not increase in that study, the authors proposed that heme may relieve BACH1-mediated repression. In palmitate-treated immortalized human renal proximal tubular epithelial cells, 5-ALA reduced BACH1 mRNA and increased HO-1 expression [14]. Heme is known to relieve BACH1-mediated repression of the HMOX1 enhancer and thereby permit Nrf2-dependent transcriptional activation [36]. Based on these previous studies, we hypothesize that Nrf2 activation and heme–BACH1 regulation may contribute to HO-1 induction mediated by 5-ALA; this signaling mechanism was not directly examined here. HO-1-derived biliverdin can additionally be converted to the antioxidant bilirubin, offering a further mechanistic link between 5-ALA and the improved redox status observed here [37].

As a heme precursor, 5-ALA may also influence mitochondrial function by supplying heme for respiratory-chain components. Ogura et al. reported increased hepatic cytochrome c oxidase activity after 5-ALA supplementation in mice [38]. Heme availability and HO-1-mediated turnover may form complementary parts of a coordinated homeostatic response. Gallio et al. showed that changes in heme availability induced coordinated responses involving heme synthesis and degradation, mitochondrial metabolism, and iron handling in HEK293 cells [39]. An increased precursor supply and heme turnover could thus jointly support heme utilization and the metabolic balance, providing a

possible explanation for the concurrent increases in HO-1 expression, the ATP content, and mitochondrial membrane potential observed here.

The network pharmacology analysis was used to generate mechanistic hypotheses and guide an interpretation of the experimental findings. Its candidates originated from multiple species, and predictions for an endogenous small molecule such as 5-ALA have limitations in species applicability and target specificity. The chicken ortholog analysis and transcriptomic overlap provide a species-relevant context for these hypotheses.

Several limitations should be considered. The fatty acid oxidation flux, mitochondrial respiration, and ultrastructure were not measured directly. Heme synthesis and degradation were also not directly quantified, leaving their relative contributions to the effects of 5-ALA unresolved. Nrf2/BACH1 signaling was not measured, and its proposed role in HO-1 induction remains a hypothesis; further work should examine this pathway and HO-1 enzymatic activity. The use of a single HMOX1-targeting siRNA leaves the possibility of sequence-specific off-target effects, and a second independent siRNA would strengthen the evidence. A rescue experiment restoring HMOX1 expression after silencing was not performed; this would strengthen the assessment of the specificity of the observed effects. In addition, LMH is a hepatoma cell line derived from a male chicken [40], whereas the laying-hen liver is subject to estrogen-dependent metabolic regulation [1]. Experiments in primary laying-hen hepatocytes would help establish how the cellular findings relate to the reproductive physiology of hens.

5. Conclusions

Dietary supplementation with 20 mg/kg 5-ALA improved hepatic lipid homeostasis in laying hens under standard production conditions, as evidenced by reduced hepatic lipid accumulation, coordinated increases in fatty acid degradation-, peroxisome-, and mitochondrial function-related markers, and enhanced HMOX1 expression. HMOX1 silencing in LMH hepatocytes partially attenuated selected protein responses and the lipid-lowering effects of 5-ALA, providing functional evidence that HO-1 contributes to the hepatocellular response. These findings position 5-ALA as a promising nutritional modulator of the hepatic lipid–redox balance in laying hens and justify further dose–response and FLHS challenge studies to support field applications.

Supplementary Materials: The following supporting information can be downloaded at: https://www.mdpi.com/article/10.3390/ani16233782/s1, Table S1, whole-blood hemoglobin concentrations (mean ± SEM); Table S2, eight overlapping chicken ortholog candidates and differentially expressed genes; Table S3, HMOX1 and CPT1A RNA-seq results and candidate sources; Table S4, human reference identifiers and chicken orthology; Table S5, candidate-source records; Table S6, SwissTargetPrediction protein-species audit; Table S7, archived SEA records; Table S8, significant chicken GO and KEGG enrichment results; Table S9, sensitivity analysis of SEA-only additions and analysis settings; original Western blot images for Figures 5–7.

Author Contributions: Conceptualization, X.W. and W.M.; Methodology, X.W. and W.M.; Validation, H.L. and L.P.; Formal analysis, X.W. and H.L.; Investigation, X.W., H.L., L.P. and D.Z.; Resources, D.Z.; Data curation, X.W. and H.L.; Writing—original draft, X.W.; Writing—review and editing, W.M.; Visualization, X.W. and L.P.; Supervision, W.M.; Project administration, W.M.; Funding acquisition, W.M. All authors have read and agreed to the published version of the manuscript.

Funding: This work was supported by the Jiangsu Modern Agriculture Key Technology Integration and Demonstration Project (No. JCTG[2025]15).

Institutional Review Board Statement: Animal experiments were conducted in accordance with the Guidelines for the Care and Use of Laboratory Animals in China and received approval from the Animal Ethics Committee at Nanjing Agricultural University (Approval NJAULLSC2024064).

Informed Consent Statement: Not applicable.

Data Availability Statement: Supporting data are provided in the Supplementary Materials.

Acknowledgments: We are grateful for the public platform provided by the Key Laboratory of Animal Physiology and Biochemistry, Ministry of Agriculture and Rural Affairs, College of Veterinary Medicine, Nanjing Agricultural University.

Conflicts of Interest: The authors declare no conflict of interest.

Abbreviations

5-ALA	5-aminolevulinic acid
ACAA1	acetyl-CoA acyltransferase 1
ACSL1	long-chain acyl-CoA synthetase 1
ALT	alanine aminotransferase
AST	aspartate aminotransferase
CE	cholesteryl ester
CON	control
COXIV	cytochrome c oxidase subunit IV
CPT1A	carnitine palmitoyltransferase 1A
FC	free cholesterol
FLHS	fatty liver hemorrhagic syndrome
GO	Gene Ontology
GSEA	gene set enrichment analysis
HO-1	heme oxygenase 1
KEGG	Kyoto Encyclopedia of Genes and Genomes
MDA	malondialdehyde
MFN2	mitofusin 2
PA/OA	palmitic acid/oleic acid
PGC-1α	peroxisome proliferator-activated receptor γ coactivator 1α
ROS	reactive oxygen species
SDHB	succinate dehydrogenase complex iron sulfur subunit B
siNC	non-targeting negative-control siRNA
SOD	superoxide dismutase
TC	total cholesterol
TFAM	mitochondrial transcription factor A
TG	triglyceride
TOM20	translocase of outer mitochondrial membrane 20
VLDLy	yolk-targeted very-low-density lipoprotein
VTG	vitellogenin

References

1. Ren, J.; Tian, W.; Jiang, K.; Wang, Z.; Wang, D.; Li, Z.; Yan, F.; Wang, Y.; Tian, Y.; Ou, K.; et al. Global investigation of estrogen-responsive genes regulating lipid metabolism in the liver of laying hens. *BMC Genom.* **2021**, *22*, 428. https://doi.org/10.1186/s12864-021-07679-y.
2. Shini, A.; Shini, S.; Bryden, W.L. Fatty liver haemorrhagic syndrome occurrence in laying hens: Impact of production system. *Avian Pathol.* **2019**, *48*, 25–34. https://doi.org/10.1080/03079457.2018.1538550.
3. Fromenty, B.; Roden, M. Mitochondrial alterations in fatty liver diseases. *J. Hepatol.* **2023**, *78*, 415–429. https://doi.org/10.1016/j.jhep.2022.09.020.
4. Jian, H.; Li, R.; Huang, X.; Li, J.; Li, Y.; Ma, J.; Zhu, M.; Dong, X.; Yang, H.; Zou, X. Branched-chain amino acids alleviate NAFLD via inhibiting de novo lipogenesis and activating fatty acid β-oxidation in laying hens. *Redox Biol.* **2024**, *77*, 103385. https://doi.org/10.1016/j.redox.2024.103385.

5. Xing, Y.; Huang, B.; Cui, Z.; Zhang, Q.; Ma, H. Dioscin improves fatty liver hemorrhagic syndrome by promoting ERα-AMPK mediated mitophagy in laying hens. *Phytomedicine* **2024**, *135*, 156056. https://doi.org/10.1016/j.phymed.2024.156056.
6. Tian, W.; Gonzales, G.B.; Wang, H.; Yang, Y.; Tang, C.; Zhao, Q.; Zhang, J.; Zhang, H.; Qin, Y. Caffeic acid and chlorogenic acid mediate the ADPN-AMPK-PPARα pathway to improve fatty liver and production performance in laying hens. *J. Anim. Sci. Biotechnol.* **2025**, *16*, 49. https://doi.org/10.1186/s40104-025-01175-z.
7. Miao, S.; Mu, T.; Li, R.; Li, Y.; Zhao, W.; Li, J.; Dong, X.; Zou, X. Coated sodium butyrate ameliorates high-energy and low-protein diet induced hepatic dysfunction via modulating mitochondrial dynamics, autophagy and apoptosis in laying hens. *J. Anim. Sci. Biotechnol.* **2024**, *15*, 15. https://doi.org/10.1186/s40104-023-00980-8.
8. Belot, A.; Puy, H.; Hamza, I.; Bonkovsky, H.L. Update on heme biosynthesis, tissue-specific regulation, heme transport, relation to iron metabolism and cellular energy. *Liver Int.* **2024**, *44*, 2235–2250. https://doi.org/10.1111/liv.15965.
9. Hendawy, A.O.; Khattab, M.S.; Sugimura, S.; Sato, K. Effects of 5-Aminolevulinic Acid as a Supplement on Animal Performance, Iron Status, and Immune Response in Farm Animals: A Review. *Animals* **2020**, *10*, 1352. https://doi.org/10.3390/ani10081352.
10. Yu, H.; Zhang, M.; Ma, Y.; Lu, J.; Pan, J.; Pan, P.; Chen, H.; Jia, W. 5-ALA ameliorates hepatic steatosis through AMPK signaling pathway. *J. Mol. Endocrinol.* **2017**, *59*, 121–128. https://doi.org/10.1530/jme-16-0260.
11. Hashimoto, T.; Sugihara, T.; Kanda, T.; Takata, T.; Isomoto, H. 5-Aminolevulinic Acid Attenuates Glucose-Regulated Protein 78 Expression and Hepatocyte Lipoapoptosis via Heme Oxygenase-1 Induction. *Int. J. Mol. Sci.* **2021**, *22*, 11405. https://doi.org/10.3390/ijms222111405.
12. Chen, J.; Wang, H.; Wu, Z.; Gu, H.; Li, C.; Wang, S.; Liu, G. Effects of 5-aminolevulinic acid on the inflammatory responses and antioxidative capacity in broiler chickens challenged with lipopolysaccharide. *Animal* **2022**, *16*, 100575. https://doi.org/10.1016/j.animal.2022.100575.
13. Nanto-Hara, F.; Ohtsu, H. Dietary 5-Aminolevulinic Acid Alleviates Heat Stress-Induced Renal Injury in Laying Hens by Improving Mitochondrial Quality and Enhancing Antioxidant Activity. *Antioxidants* **2025**, *14*, 556. https://doi.org/10.3390/antiox14050556.
14. Hamada, S.; Mae, Y.; Takata, T.; Hanada, H.; Kubo, M.; Taniguchi, S.; Iyama, T.; Sugihara, T.; Isomoto, H. Five-Aminolevulinic Acid (5-ALA) Induces Heme Oxygenase-1 and Ameliorates Palmitic Acid-Induced Endoplasmic Reticulum Stress in Renal Tubules. *Int. J. Mol. Sci.* **2023**, *24*, 10151. https://doi.org/10.3390/ijms241210151.
15. Daina, A.; Michielin, O.; Zoete, V. SwissTargetPrediction: Updated data and new features for efficient prediction of protein targets of small molecules. *Nucleic Acids Res.* **2019**, *47*, W357–W364. https://doi.org/10.1093/nar/gkz382.
16. Kolberg, L.; Raudvere, U.; Kuzmin, I.; Adler, P.; Vilo, J.; Peterson, H. g:Profiler—Interoperable web service for functional enrichment analysis and gene identifier mapping (2023 update). *Nucleic Acids Res.* **2023**, *51*, W207–W212. https://doi.org/10.1093/nar/gkad347.
17. National Research Council. *Nutrient Requirements of Poultry*, 9th rev. ed.; The National Academies Press: Washington, DC, USA, 1994. https://doi.org/10.17226/2114.
18. Chang, X.; Wang, B.; Zhang, H.; Qiu, K.; Wu, S. The change of albumen quality during the laying cycle and its potential physiological and molecular basis of laying hens. *Poult. Sci.* **2024**, *103*, 104004. https://doi.org/10.1016/j.psj.2024.104004.
19. Kleiner, D.E.; Brunt, E.M.; Van Natta, M.; Behling, C.; Contos, M.J.; Cummings, O.W.; Ferrell, L.D.; Liu, Y.-C.; Torbenson, M.S.; Unalp-Arida, A.; et al. Design and validation of a histological scoring system for nonalcoholic fatty liver disease. *Hepatology* **2005**, *41*, 1313–1321. https://doi.org/10.1002/hep.20701.
20. Chen, Y.J.; Cho, J.H.; Yoo, J.S.; Wang, Y.; Huang, Y.; Kim, I.H. Evaluation of δ-Aminolevulinic Acid on Serum Iron Status, Blood Characteristics, Egg Performance and Quality in Laying Hens. *Asian-Australas. J. Anim. Sci.* **2008**, *21*, 1355–1360. https://doi.org/10.5713/ajas.2008.70634.
21. Wang, J.P.; Lee, J.H.; Jang, H.D.; Yan, L.; Cho, J.H.; Kim, I.H. Effects of δ-aminolevulinic acid and vitamin C supplementation on iron status, production performance, blood characteristics and egg quality of laying hens. *J. Anim. Physiol. Anim. Nutr.* **2011**, *95*, 417–423. https://doi.org/10.1111/j.1439-0396.2010.01067.x.
22. Menezes, P.R.; González, C.B.; DeSouza, A.O.; Maria, D.A.; Onuki, J. Effect of 5-aminolevulinic acid on the expression of carcinogenesis-related proteins in cultured primary hepatocytes. *Mol. Biol. Rep.* **2018**, *45*, 2801–2809. https://doi.org/10.1007/s11033-018-4367-5.
23. Hu, H.; Huang, Y.; Li, A.; Mi, Q.; Wang, K.; Chen, L.; Zhao, Z.; Zhang, Q.; Bai, X.; Pan, H. Effects of different energy levels in low-protein diet on liver lipid metabolism in the late-phase laying hens through the gut-liver axis. *J. Anim. Sci. Biotechnol.* **2024**, *15*, 98. https://doi.org/10.1186/s40104-024-01055-y.

24. Liang, K. Mitochondrial CPT1A: Insights into structure, function, and basis for drug development. *Front. Pharmacol.* **2023**, *14*, 1160440. https://doi.org/10.3389/fphar.2023.1160440.
25. Tahri-Joutey, M.; Andreoletti, P.; Surapureddi, S.; Nasser, B.; Cherkaoui-Malki, M.; Latruffe, N. Mechanisms Mediating the Regulation of Peroxisomal Fatty Acid Beta-Oxidation by PPARα. *Int. J. Mol. Sci.* **2021**, *22*, 8969. https://doi.org/10.3390/ijms22168969.
26. Grevengoed, T.J.; Klett, E.L.; Coleman, R.A. Acyl-CoA Metabolism and Partitioning. *Annu. Rev. Nutr.* **2014**, *34*, 1–30. https://doi.org/10.1146/annurev-nutr-071813-105541.
27. Pfanner, N.; Warscheid, B.; Wiedemann, N. Mitochondrial proteins: From biogenesis to functional networks. *Nat. Rev. Mol. Cell Biol.* **2019**, *20*, 267–284. https://doi.org/10.1038/s41580-018-0092-0. Correction in *Nat. Rev. Mol. Cell Biol.* **2021**, *22*, 367. https://doi.org/10.1038/s41580-021-00361-x.
28. Yao, H.; Hu, Y.; Tong, H.; Shi, S. Dimethylglycine Alleviates Metabolic Dysfunction-Associated Fatty Liver Disease by Improving the Circulating Estrogen Level via Gut *Staphylococcus*. *J. Agric. Food Chem.* **2024**, *72*, 2708–2717. https://doi.org/10.1021/acs.jafc.3c07075.
29. Chu, Y.; Zhao, J.; Zhao, Y.; Li, Z.; Yang, S.; Chen, N.; Liu, Y.; Zhang, J.; Zhou, L.; Chen, X. Multi-Omics Reveal the Effects and Regulatory Mechanism of Dietary Magnolol Supplementation on Production Performance of Post-Peak Laying Hens. *J. Agric. Food Chem.* **2025**, *73*, 4027–4041. https://doi.org/10.1021/acs.jafc.4c07245.
30. Wang, Y.; Gong, P.; Zhao, S.; He, F.; Ma, H. (−)-Epicatechin Protects against Fatty Liver Hemorrhagic Syndrome in Laying Hens by Integrating Multitarget Mechanisms via ERα Signaling. *J. Agric. Food Chem.* **2026**, *74*, 18051–18071. https://doi.org/10.1021/acs.jafc.6c04072.
31. Li, L.; Hao, J.; Zhang, C.; Li, Y.; Wang, Y.; Feng, J.; Hu, C. Effects of fermented feed from broccoli stems and leaves on growth performance, gut microbiota and carcass quality of Jinhua pigs. *Anim. Nutr.* **2026**, *3*, e12. https://doi.org/10.1017/anr.2026.10032.
32. Goicoechea, L.; Conde de la Rosa, L.; Torres, S.; García-Ruiz, C.; Fernández-Checa, J.C. Mitochondrial cholesterol: Metabolism and impact on redox biology and disease. *Redox Biol.* **2023**, *61*, 102643. https://doi.org/10.1016/j.redox.2023.102643.
33. Listenberger, L.L.; Han, X.; Lewis, S.E.; Cases, S.; Farese, R.V., Jr.; Ory, D.S.; Schaffer, J.E. Triglyceride accumulation protects against fatty acid-induced lipotoxicity. *Proc. Natl. Acad. Sci. USA* **2003**, *100*, 3077–3082. https://doi.org/10.1073/pnas.0630588100.
34. Mashek, D.G. Hepatic lipid droplets: A balancing act between energy storage and metabolic dysfunction in NAFLD. *Mol. Metab.* **2021**, *50*, 101115. https://doi.org/10.1016/j.molmet.2020.101115.
35. Huang, C.; Gao, X.; Shi, Y.; Guo, L.; Zhou, C.; Li, N.; Chen, W.; Yang, F.; Li, G.; Zhuang, Y.; et al. Inhibition of Hepatic AMPK Pathway Contributes to Free Fatty Acids-Induced Fatty Liver Disease in Laying Hen. *Metabolites* **2022**, *12*, 825. https://doi.org/10.3390/metabo12090825.
36. Sun, J.; Hoshino, H.; Takaku, K.; Nakajima, O.; Muto, A.; Suzuki, H.; Tashiro, S.; Takahashi, S.; Shibahara, S.; Alam, J.; et al. Hemoprotein Bach1 regulates enhancer availability of heme oxygenase-1 gene. *EMBO J.* **2002**, *21*, 5216–5224. https://doi.org/10.1093/emboj/cdf516.
37. Barañano, D.E.; Rao, M.; Ferris, C.D.; Snyder, S.H. Biliverdin reductase: A major physiologic cytoprotectant. *Proc. Natl. Acad. Sci. USA* **2002**, *99*, 16093–16098. https://doi.org/10.1073/pnas.252626999.
38. Ogura, S.-I.; Maruyama, K.; Hagiya, Y.; Sugiyama, Y.; Tsuchiya, K.; Takahashi, K.; Abe, F.; Tabata, K.; Okura, I.; Nakajima, M.; et al. The effect of 5-aminolevulinic acid on cytochrome c oxidase activity in mouse liver. *BMC Res. Notes* **2011**, *4*, 66. https://doi.org/10.1186/1756-0500-4-66.
39. Gallio, A.E.; Marson, N.A.; Heesom, K.J.; Lewis, P.A.; Alibhai, D.; Dugdale, C.A.; Herman, A.; Basran, J.; Hudson, A.J.; Raven, E.L. An extended network for regulation of heme homeostasis in cells. *Proc. Natl. Acad. Sci. USA* **2025**, *122*, e2508237122. https://doi.org/10.1073/pnas.2508237122.
40. Kawaguchi, T.; Nomura, K.; Hirayama, Y.; Kitagawa, T. Establishment and characterization of a chicken hepatocellular carcinoma cell line, LMH. *Cancer Res.* **1987**, *47*, 4460–4464.

Disclaimer/Publisher's Note: The statements, opinions and data contained in all publications are solely those of the individual author(s) and contributor(s) and not of MDPI and/or the editor(s). MDPI and/or the editor(s) disclaim responsibility for any injury to people or property resulting from any ideas, methods, instructions or products referred to in the content.